Available online at www.sciencedirect.com
SCIENCE DIRECT®
Sensors and Actuators B 104 (2005) 237–248
SENSORS AND ACTUATORS B CHEMICAL
www.elsevier.com/locate/snb

Airborne analyte detection with an aircraft-adapted surface plasmon resonance sensor system

Alexei N. Naimushin[a], Charles B. Spinelli[c], Scott D. Soelberg[a], Tobias Mann[a], Richard C. Stevens[a], Timothy Chinowsky[b], Peter Kauffman[b], Sinclair Yee[b], Clement E. Furlong[a,*]

[a] *Departments of Genome Sciences and Medicine, Division of Medical Genetics, Box 357720, Seattle, WA 98195-7720, USA*
[b] *Department of Electrical Engineering, University of Washington, Seattle, WA 98195, USA*
[c] *10424 Brackenwood Lane, Bainbridge Island, WA 9810, USA*

Received 14 May 2004; accepted 18 May 2004
Available online 2 September 2004

Abstract

A portable surface plasmon resonance (SPR) biosensor system was designed for deployment in a surrogate unmanned aerial vehicle (UAV). The nose of the aircraft was fitted with two nozzles for release of analytes during flight. Ovalbumin and horseradish peroxidase were chosen as simulants for airborne toxic proteins. The two protein analytes were released sequentially from the nozzles as aerosols with low concentrations of analytes during the ground test and each of three flights. A two-stage collector accumulated the sample prior to de-aeration and monitoring by the SPR system. An automated liquid handling unit directed buffer, sample, amplification and regeneration solutions to the sensor and metered the flow rate. Following detection of analyte, secondary antibodies were pumped through the sensor to both amplify and verify analyte detection, thus avoiding false positive detection and at the same time achieving higher sensitivity with the system. Analyte concentrations varied from 1 to 10 nM and the altitude at which the detection was performed varied from 1800 to 10,000 feet. All analyte releases during the three flights were successfully detected and verified. Flight parameters, such as airspeed, altitude, position and meteorological conditions, data necessary for UAV applications, were automatically recorded. The aircraft flight path obtained by GPS was temporally aligned with the SPR detection signal, allowing mapping of the geographical distribution of analyte release. The results reported here illustrate the usefulness of the portable aircraft-mounted SPR system for detection of airborne analytes.

Keywords: Biosensor; Surface plasmon resonance; Biological warfare agent; Airborne detection

1. Introduction

Accurate early detection and identification of chemical and biological warfare (CBW) agents are important components of military operations [1–4]. Civilian defense efforts face similar challenges, as many of the CBW agents can be easily produced and dispersed by terrorists. Early notification of CBW agent use provides time to develop an appropriate response to the threat—avoiding the contaminated territory, initiating decontamination, donning protective gear and generally preparing for containment of the threat. However, such plans can only be made if the threat agents are detected, identified, and accurately mapped. One of the most effective ways of dissemination of CBW agents is by aerosols [2]. Detection and mapping of aerosolized agents requires mobile sensors or an array of sensors covering the territory of interest. Deployment of ground-based sensors poses problems in rugged terrain or in areas occupied by unfriendly forces. A CBW sensor with real-time or near-real-time detection capability mounted on an unmanned aerial vehicle (UAV) would allow surveying large areas in short periods of time.

Recognizing the problem, researchers from Naval Research Laboratory mounted a fiber optic biosensor (Analyte 2000) on a UAV and used it for detection of a BW agent simulant during a 20 min flight [5,6]. Here we describe airborne detection performed by an aircraft-mounted surface plasmon resonance (SPR) biosensor system.

SPR-based sensors depend on the change of refractive index on the surface of the gold sensor element when an analyte is bound. A detailed description of the theory and

* Corresponding author. Tel.: +1-206-543-1193; fax: +1-206-543-3050.
E-mail address: clem@u.washington.edu (C.E. Furlong).

0925-4005/$ – see front matter © 2004 Elsevier B.V. All rights reserved.
doi:10.1016/j.snb.2004.05.020

practice of SPR techniques is provided in a book edited by Davies [7]. SPR biosensors have been used in research laboratories for several decades. Specificity is provided to the SPR sensor elements by immobilizing analyte-specific antibodies on each channel of the sensor elements. Binding of target analytes results in a change in the refractive index at the gold sensor surface resulting in a shift of the SPR reflectivity curve which the system software converts into a plot of refractive index as a function of time.

Standard applications of SPR-based biosensors include studies of inter-molecular interactions and drug discovery [8–10]. Recently, SPR has been used to test for food toxins and detection of BW agents [11,12]. SPR-based sensors offer several advantages over other detection methods: (1) SPR biosensors are able to provide continuous real-time monitoring. A large number of negative samples (i.e. not containing the analyte of interest) can be processed without the need for regenerating the detection chemistry or changing the sensor configuration. (2) Following analyte detection, the sensor can usually be reset by removing the target analyte with a low pH wash step [12–14]. (3) SPR sensors are universal detectors, since they can detect both BW and CW agents with the same instrument. (4) Direct detection with SPR sensors does not continuously consume reagents, unlike the majority of other detection procedures, such as enzyme linked imunosorbent assays (ELISA) [15–18], light addressable potentiometric sensors (LAPS) [19–21], array biosensors [17,22,23], immunomagnetic separation coupled with electro-chemiluminescence and fluorescence procedures (IMS-ECL and IMS-FCL) [18,24–26] or rapid chromatographic assays (RCA) [14], all of which require the additional analytes used in sandwich assays. In addition to a direct detection mode, SPR biosensors can also work in an amplification mode to further lower the detection limit. This is accomplished using antibodies for amplification at a minimal cost for reagent consumption. (5) Compactness of the Spreeta SPR sensor components manufactured by Texas Instruments (TI, Dallas, TX) makes them prime candidates for use in the development of portable systems for field use, especially when outfitted with a temperature control module and one or more reference channels [12].

Given the advantages of the SPR biosensors, we decided to test the feasibility of airborne detection using an aircraft-mounted SPR-based system. Additionally, we wanted to test such parameters as ruggedness of the system, sensor response under varying pressure and temperature, detection limits as well as the adaptability of the system and protocols to different platforms. Since our SPR sensor system weighs less than the Analyte 2000 system, it could easily be mounted on an UAV platform for unmanned detection. Through modifications described below, we adapted a previously described temperature controlled SPR system [12,27] for use in an experimental aircraft. The aircraft was then used for detection of two innocuous proteins that we chose as simulants of toxic protein BW agents. Detection experiments were performed during one ground test and three separate flights at several altitudes from 1800 to 10,000 feet. In addition to bio-detection data, meteorological and flight data were recorded. Position of the aircraft was tracked with global position system (GPS) detectors and synchronized to the collected detection data. Combining detection data with airplane position data provided a system for geographical mapping of analyte distribution. To our knowledge, the experiments described here demonstrate the first use of SPR aircraft-mounted sensors for airborne analyte detection.

2. Experimental

2.1. Aircraft

The aircraft used as a surrogate unmanned aerial vehicle was an experimental tandem-seat, pusher-prop designed by Burt Rutan and piloted by Charles Spinelli. The Vari-Viggen (Figs. 1 and 2) is an all-wood fuselage, composite delta wing with fully retractable landing gear. The aircraft is ideal for use as a surrogate UAV platform for a variety of reasons. The aircraft can fly a wide range of airspeeds and has superb handling characteristics at low airspeeds and high angles of attack (AOA). The pusher-prop design provided mounting locations for the air sample collection devices where the airflow was undisturbed by the propeller and was free of engine contaminates. The sensor electronics and operator were located a short distance from the sample collection port (Fig. 3) and equipment was easily accessible by the operator. This made the Vari-Viggen a very capable and flexible platform for simulating the environment airborne sensors would encounter on an UAV platform.

Sensors were integrated into the aircraft as shown in Fig. 2. A fiberglass air sample collection port with two forward mounted analyte ejection nozzles was fabricated and mounted on the nose of the aircraft (Fig. 3). The sensor electronics and fluidics were mounted in the aft passenger compartment. Power was supplied by the aircraft electrical system.

The aircraft was instrumented with state of the art avionics that included an electronic flight instrumentation system (EFIS),[1] two global positioning system (GPS) receivers,[2] a 2-axis automated flight control system[3] (AFCS) and two humidity/temperature data loggers. The AFCS is designed so that the pilot can load and fly pre-programmed flight profiles or use controls on the hands-on throttle and stick (HOTAS) to command roll and pitch changes to the AFCS. The AFCS can also be controlled remotely from a ground station when a telemetry system and the flight guidance control computer (FGCC), features in common with UAVs.

[1] Dynon Development EFIS D-10.
[2] Lowrance Avioncs AirMap 300, Bendix King KLX-135.
[3] S-tec System 60-2 Roll and Pitch Flight Guidance Computers Modified for UAV use.

Fig. 1. Photograph of the experimental two-seater, pusher-prop Vari-Viggen aircraft with mounted SPR sensor, its pilot and its sensor operator.

Data from these instruments were synchronized to a GPS time stamp and recorded on a laptop computer. The data set included the EFIS high data rate (64 Hz) Universal Time (UTC or GMT, Greenwich Mean Time) time, attitude, airspeed, altitude, turn rate, angle of attack, vertical G's and lateral G's. The 1 Hz data set included the GPS, UTC time, position, ground speed, magnetic course, figure of merit and the data logger output UTC time, humidity and temperature. During post-flight analysis, the time stamps were aligned and additional data were derived which included wind speed and direction, true airspeed and climb/descent rates.

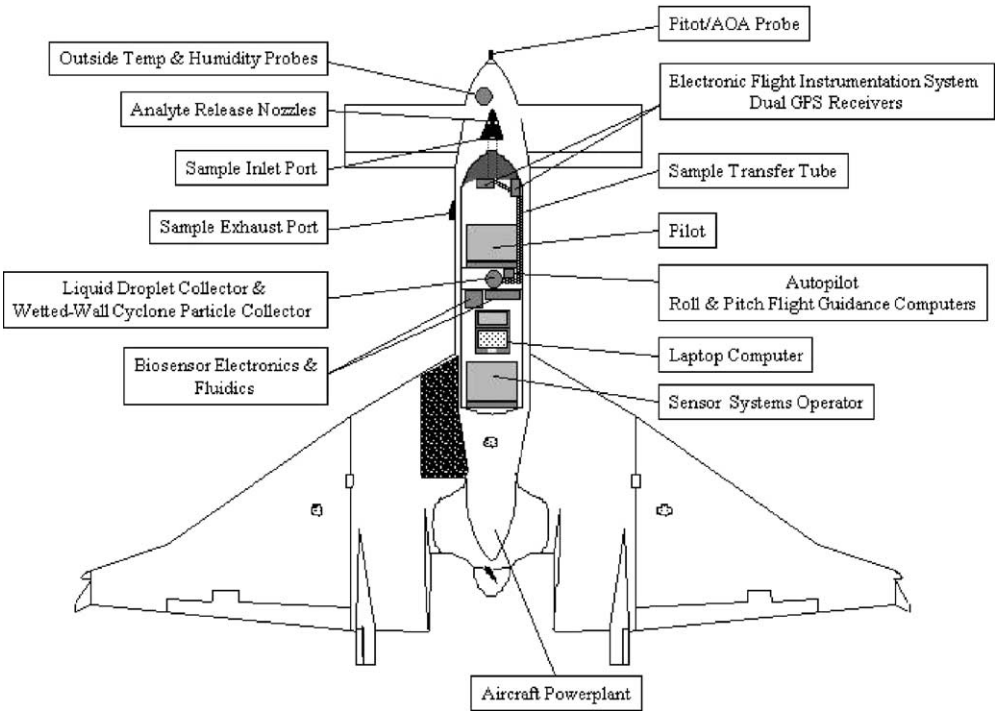

Fig. 2. Aircraft equipment layout.

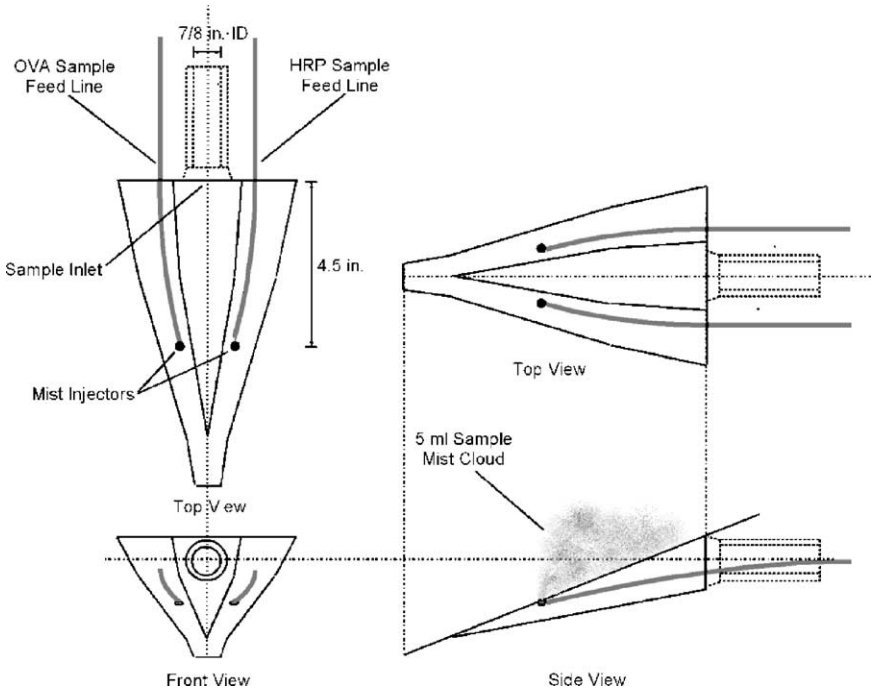

Fig. 3. Diagram of sample release nozzles and pickup port located in front of the cockpit of the aircraft as noted in Fig. 2.

Aircraft specifications

Wing span	23.7 feet
Wing area	125 feet^2
Length	20 feet
Height	6.1 feet
Cabin dimensions	9.1 feet × 2 feet
Crew	Two, single pilot operation
Empty weight	1136 lb
Gross weight	1860 lb
Useful load	724 lb
Fuel capacity	25 gal main, 13.7 gal aux
Electrical power	35 A at 12 V dc, 420 W
Propulsion	180 hp Lycoming O-360-AID
Maximum speed	180 mph
Minimum speed	65 mph
Climb rate (sea level)	1500 fpm
Maximum altitude	20000 feet MSL
Endurance	4.5 h

2.2. Biosensor electronics

The core of the instrument consisted of two SPR sensor modules (Texas Instruments' Spreeta devices) attached to digital signal processing (DSP) hardware and a laptop computer, which controlled the sensors and acquired sensor data [12,27]. A diagram of the SPR sensor element is shown in Fig. 6A. To reduce measurement disturbances due to temperature, the sensors and fluids entering the sensor were temperature controlled, reducing variations to less than ±0.1 C.

2.3. Fluidics

The sensor system's semi-automated fluid handling unit was designed for ease of use, while still allowing the operator to make changes during the time course of the experiment. A schematic illustration of the fluidics system is shown in Fig. 4. A computer-controlled rotary valve enabled the user to choose between various fluid sources. Initially, the valve directed the buffer solution to the sensor for establishment of a baseline. For direct detection of analytes present in the sample, the valve channeled sample collected from the liquid gravity trap to the sensor. To verify the detection and amplify the detection response, solution containing specific secondary antibodies was directed through the sensor. This amplification solution was followed by buffer solution to establish the overall magnitude of the SPR response. To return the sensor back to operational condition, a low pH regeneration solution was used to remove analytes from the sensor surface. An in-line degasser (Fig. 5) removed bubbles and degassed solutions immediately prior to their entry into the sensor flowcells. Laser-cut mylar flowcells (Fig. 7) adhered to the sensor surfaces directed the flow of liquid analyte across all channels of the sensor surface. An outlet pump metered the flow rate of liquids through the sensor system.

2.4. Sample collection

A two part sample collection system consisting of a gravity droplet collector followed by a particle collector system was in place upstream of the sensor system. The intake port was located on the nose of the aircraft (Figs. 2 and 3).

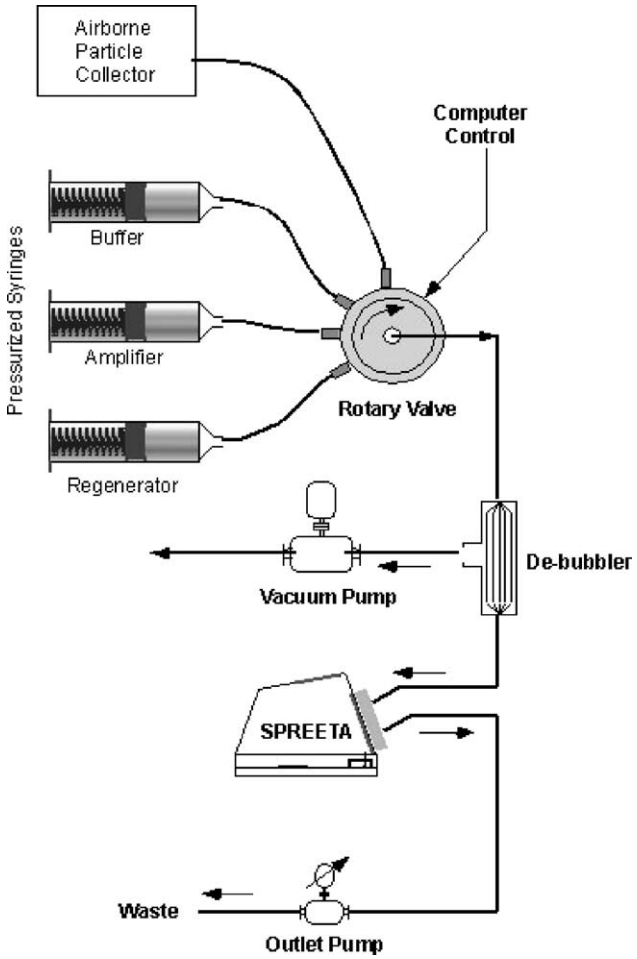

Fig. 4. Schematic diagram of sensor fluidics. The computer-controlled rotary valve selected appropriate analyte, which traveled through the debubbler before being introduced into SPR sensor flowcell. The exit pump metered the flow.

A smooth polyethylene tube (16 mm i.d.) linked the intake port to the collector located inside the crew compartment. The two-part sample collector consisted of a custom gravity droplet collector, followed by a wetted-wall cyclone particle collector (SASS 2000, Research International, Monroe, WA). The collector's fan drew air and liquid sample through the collection tubing, and into the liquid collector. Liquid droplets in the sample fell into the gravity droplet collector, while airflow continued into the particle collector. The depleted air stream then exited through a port in the side of the aircraft. The SASS 2000 provided airflow for the ground testing. It was flown as part of the system to test its suitability as a particle collector for future flights. For the three flights described here, the released protein analytes were recovered from the gravity droplet collector.

This two-stage collection process eliminates dilution of any collected liquid samples by the fluid resident in the particle collector.

After leaving the gravity droplet collector, liquid sample flowed through a debubbler/deaerator apparatus (Fig. 5). Due to their nature, air collectors produce highly aerated samples which are prone to bubble formation. Bubbles on the sensor surface interfere with SPR measurements and must be eliminated. The debubbler consisted of a bundle of gas-permeable hollow fibers with 220–230 μm i.d. and 30 nM pore size (Fig. 5). When vacuum was applied to the debubbler, bubbles and dissolved gases were drawn out of the pores in the hollow fibers, leaving a degassed sample stream.

2.5. Sample release method

Rather than creating large plumes of samples through which the aircraft could fly, we released small quantities of liquid sample from the spray nozzles located on the nose of the aircraft forward of the collector inlet (Figs. 2 and 3). The goal of this project was to detect analytes simulating airborne BW agents in the forms in which they are likely to be deployed, in this case simulants of aerosols of protein toxins. The SASS 2000 particle collector is designed to collect dry particles of the size that have been found to be most effective for airborne biological weapons. For these experiments, we analyzed samples consisting of fine mist of analytes in aqueous form.

2.6. Choice of detection targets

Two non-toxic proteins, ovalbumin (OVA) and horseradish peroxidase (HRP), purchased from Sigma (St. Louis, MO), were chosen as BW simulants for these experiments, based on the commercial availability of both proteins and antibodies to these proteins. Protein A purified polyclonal antibodies to OVA and HRP were from Biodesign, Intl. (Saco, ME). The antibodies to the OVA and HRP proteins were affinity purified using an AminoLink Plus Immobilization Kit from Pierce Biotechnology (Rockford, IL). The procedures for coupling the proteins to the columns and affinity purification of the antibodies were taken directly from the instructions provided with the kit. Briefly, the affinity resin contained in a 2 ml column was mixed with a 10 mg/ml solution of the HRP or OVA in pH 7.2 coupling buffer overnight. The excess solution was eluted from the column, which was then was rinsed with 10 column volumes of PBS (0.1 M sodium phosphate, 0.15 M NaCl, pH 7.2). Any remaining active sites were blocked by eluting the column with 5 column volumes of 1 M Tris–HCl, 0.05% NaN_3, pH 7.4. The column was equilibrated in PBS prior to use. A 2.5 ml of a solution of 10 mg/ml rabbit anti-OVA or sheep anti-HRP was added to each column, followed by a column rinse step with 20 ml PBS. The columns were eluted with 8 ml of 100 mM glycine, pH 2.2 and 1 ml fractions were collected directly into 100 μl of 1 M Tris–HCl buffer, pH 9.5. The collected samples were dialyzed overnight in PBS. Absorbance at 280 nm indicated a 2 mg/ml final concentration of anti-OVA (2 ml) and a 1 mg/ml concentration of anti-HRP (2 ml).

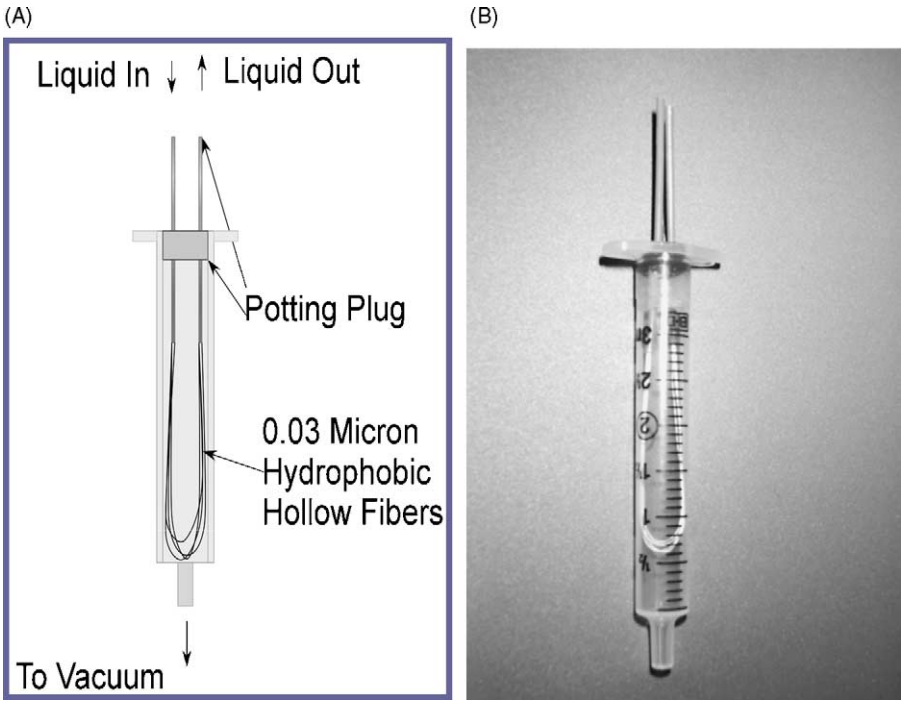

Fig. 5. A schematic diagram (A) and a photograph (B) of the 0.03 μm pore size hollow-fiber debubbler/degasser.

2.7. Sensor functionalization

Sensor surface functionalization involved a multi-step process that prepared the surface for specific detection applications. Gold binding peptide (GBP) bound to the gold sensor surface formed the foundation layer to which the antibodies were covalently attached [12,28]. Each sensor was cleaned and pre-functionalized according to the following protocol. (1) The gold surface was cleaned with acetone and then ethanol using lens paper to remove residues and dust particles. (2) A stencil, laser cut from adhesive-backed mylar (Fralock Corporation, Canoga Park, CA), was attached to each sensor to allow functionalization chemistry to be applied to each channel independently (Fig. 6). (3) Next, 500 μl of 20 μg/ml GBP-AP solution in PKT-50 (10 mM KH_2PO_4, 50 mM KCl, 1% Triton X-100, pH 7.0) was added, covering all channels, and allowed to sit for 30 min. (4) Slides were rinsed in ddH_2O, then incubated for 30 min with 50 μg/ml trypsin (Sigma St. Louis, MO) in 10 mM Tris, 10 mM $CaCl_2$, pH 8.0 buffer. Trypsin cleaved the alkaline phosphatase domain from the gold binding peptide domain, leaving the gold-binding domain as a foundation layer on the gold sensor surface [28]. (5) The slides were rinsed with ddH_2O, then incubated in a 50 μg/ml trypsin inhibitor (Sigma, St. Louis, MO) solution for 30 min to inhibit any further trypsin action. (6) Steps 3–5 were repeated to ready the sensor for antibody attachment.

Antibodies for the target antigen were covalently attached to the GBP foundation layer. The carboxyl groups on the GBP were activated using standard EDC (1-ethyl-3-[3-dimethylaminopropyl]carbodiimide hydrochloride), *S*-NHS (*N*-hydroxysulfosuccinimide) chemistry [29,30]. EDC (100 mg) from Pierce (Rockford, IL) and S-NHS (27.5 mg) from Fluka (Milwaukee, WI) were dissolved in 5 ml H_2O, then 500 μl of this solution was used to cover the sensor surface for 30 min. The surface was then rinsed with ddH_2O. To slow the hydrolysis of active esters present after the addition of EDC and *S*-NHS, 10 mM Na^+ acetate at pH 5.0 was used as a buffer. The antibodies were coupled to the carboxyl-activated GBP foundation layer by carefully adding 8 μl of a 250 μg/ml antibody solution in 10 mM Na^+ acetate buffer to the individual channels, defined by the stencil (Fig. 6B). After 30 min the channels were rinsed with double distilled water (ddH_2O). The sensor surfaces were then covered with 8 μl of storage buffer (2.5% trehalose/2.5% dextran), allowed to dry and stored at 4 °C until used. Shortly before use, the mylar stencil functionalization mask was removed and replaced with a mylar flow cell gasket with a single opening for both of the channels. The gasket formed both the seal and flow channel of the flow cell (Fig. 7). The plastic (Delrin) cover forming the top of the flowcell was drilled and tapped for standard HPLC fittings.

3. Results and discussion

One ground test and three flights were carried out to evaluate the performance of the SPR-based sensor system for detection of airborne analytes. The ground test showed detection of both analytes released as mists of 10 nM aqueous solutions. The ground test also revealed that temperature-regulated aluminum sensor enclosure needed to be further insulated to avoid temperature variations due to changes in cabin temperature.

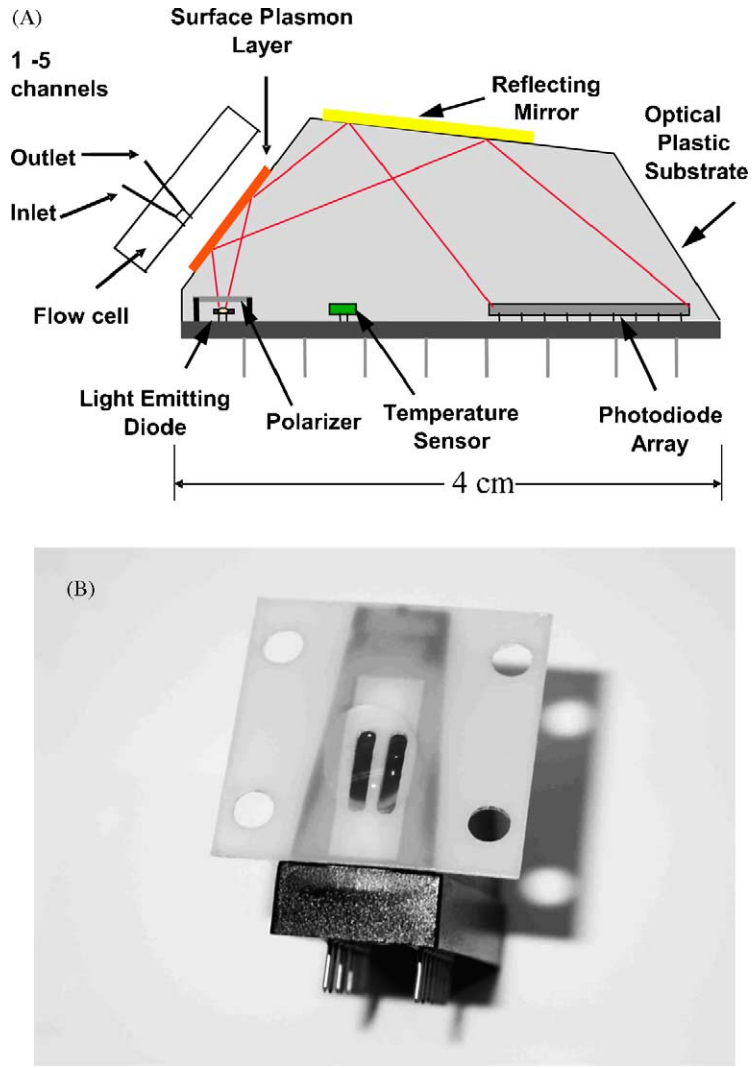

Fig. 6. (A) Diagram of the Spreeta sensor module. (B) Mylar mask with two wells used to functionalize the individual channels of the SPR sensors. This picture depicts the first step in the functionalization process where both channels are derivatized with GBP. Antibodies are added in smaller volumes which are contained in each well.

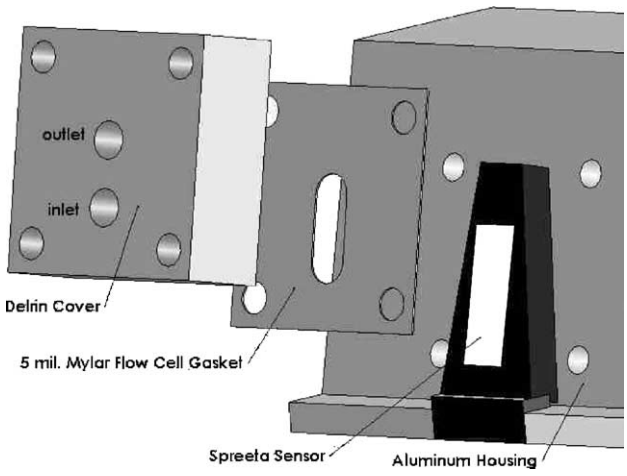

Fig. 7. Diagram of flow cell module.

Pre-testing of the debubbler/deaerator apparatus indicated that it efficiently removed bubbles as well as dissolved gas from the flow stream (Fig. 8). A dissolved oxygen sensor (Diamond General, Inc., Ann Arbor, MI) was used to measure a solution of PBS pumped through the debubbler/deaerator under vacuum. The percent O_2 of the buffer (PBS), relative to the initial concentration, was measured and used as an indicator of the total aeration of the solution. By comparison, a solution of PBS degassed in a 690 mm Hg vacuum for 100 min was still 68% DO. Large bubbles that were intentionally introduced into the flow stream were efficiently removed by the debubbler/deaerator apparatus.

During the first flight, the aircraft circled at an altitude of 1800 feet and the concentration of both analytes released was again 10 nM. An 8 min detection of OVA was followed by a 7 min amplification/verification step and a 13 min detection of HRP was followed by a 10 min amplification/verification step (Fig. 9). At time $t = 10$ min, 5 ml of ovalbumin solution

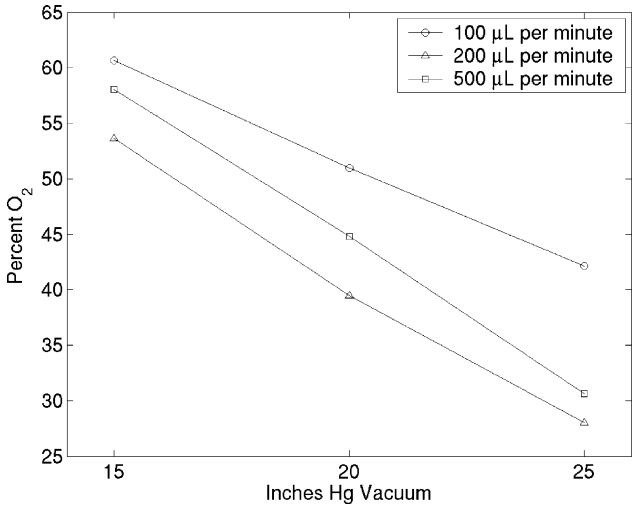

Fig. 8. Debubbler/degasser performance. Aerated PBS was flowed through the hollow fiber device (as shown in Fig. 3) under three different vacuum settings and three different flow rates. Dissolved O_2 was measured before and after flow through the device. The plot shown here indicates the % DO after flowing through the hollow fiber device, measured as a % of the starting DO value.

at a concentration of 10 nM was dispensed at the ejection nozzle outside the aircraft. There was a 3 min delay between sample injection and sensor response. The delay was due to sample travel time in the air collection and fluidic systems. (Redesign of the system for UAV applications will significantly shorten the lag between sample acquisition and signal detection. The delay between injection and detection is only 10 s in our current laboratory bench-top prototype system.) Five minutes after the release of OVA ($T = 21$ min.), amplification solution was flowed through the sensor, amplifying and verifying presence of OVA. The generated signal was very strong, which meant that detection of much smaller amount of ovalbumin would be easily achievable. The sensor was switched to the buffer solution at time $t = 29$ min. At time $t = 30$ min, the valve was switched back to intake sample and the HRP analyte was released from the nozzle. Because some residual OVA was still present in the tubing, it generated a response in its channel (black line) at the start of the HRP injection. Since the OVA channel was used as a reference channel for the HRP detection, this resulted in a non-detect initially because of subtraction of the positive values from the OVA channel (Fig. 9C). After a short time, however, the residual OVA washed through, resulting in a positive signal from the HRP channel (functionalized with anti-HRP antibodies). The HRP signal was then verified and amplified by injection of anti-HRP antibodies 5 min after the HRP injection ($t = 45$ min). The anti-HRP functionalized channel is shown in gray (Fig. 9A). In order to achieve clean referencing, an independent reference channel that does not recognize any anticipated targets is required. Future sensors will have three channels per sensor element, making possible two-analyte detection with one reference channel. The response of the biosensor obtained during the

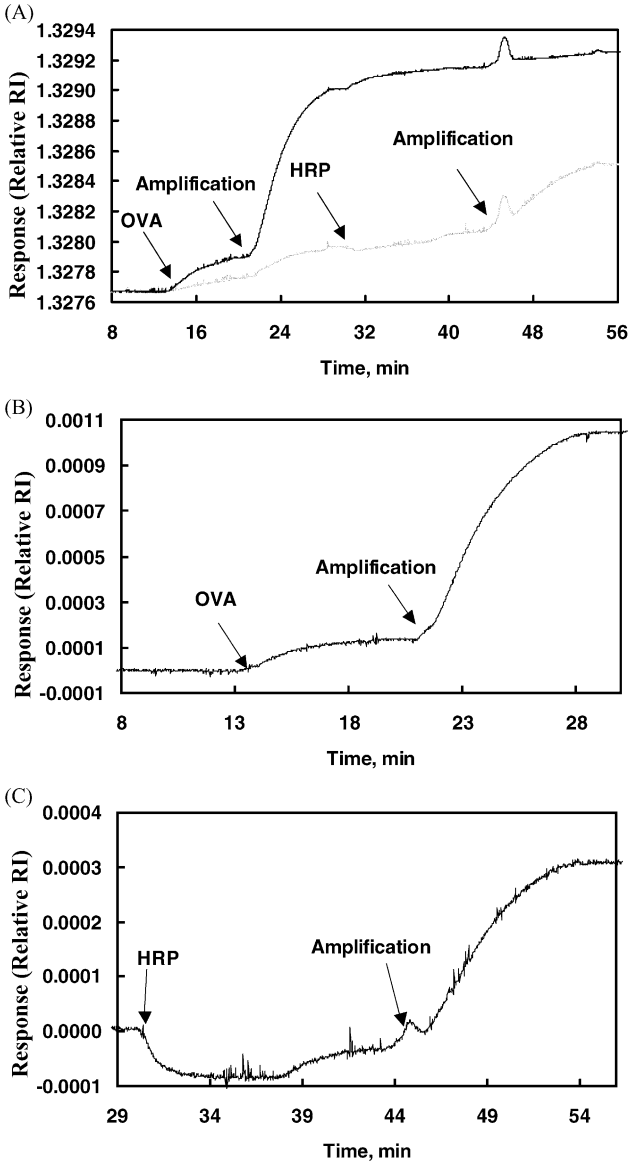

Fig. 9. Detection of ovalbumin (OVA) and horseradish peroxidase (HRP) during the first flight. Response refers to relative refractive index units. (A) Detection of each analyte as labeled. (B) Reference compensated response of anti-OVA channel. OVA was released at time $t = 10$ min. It reached the sensor surface at time $t = 13$ min. Amplification was started at time $t = 21$ min. The sensor was washed with the buffer at time $t = 29$ min. (C) Reference compensated response of anti-HRP channel. HRP was introduced at time $t = 30$ min. At time $t =$ approximately 33 min it reached the sensor. At time $t = 40$ min amplification solution was introduced. The sensor was washed with the buffer solution at time $t = 53$ min.

first flight also indicated that much lower amounts of protein toxins should be detectable. Additional amplification steps will allow improving limits of detection (LOD) even further. We have previously detected *Staphylococcus* B enterotoxin (SEB) at a concentration of 100 fM, albeit with longer analyte accumulation times [12]. The current lower level of direct detection of SEB with our laboratory SPR system is 100 pM in less than 10 min. We have also detected ricin A

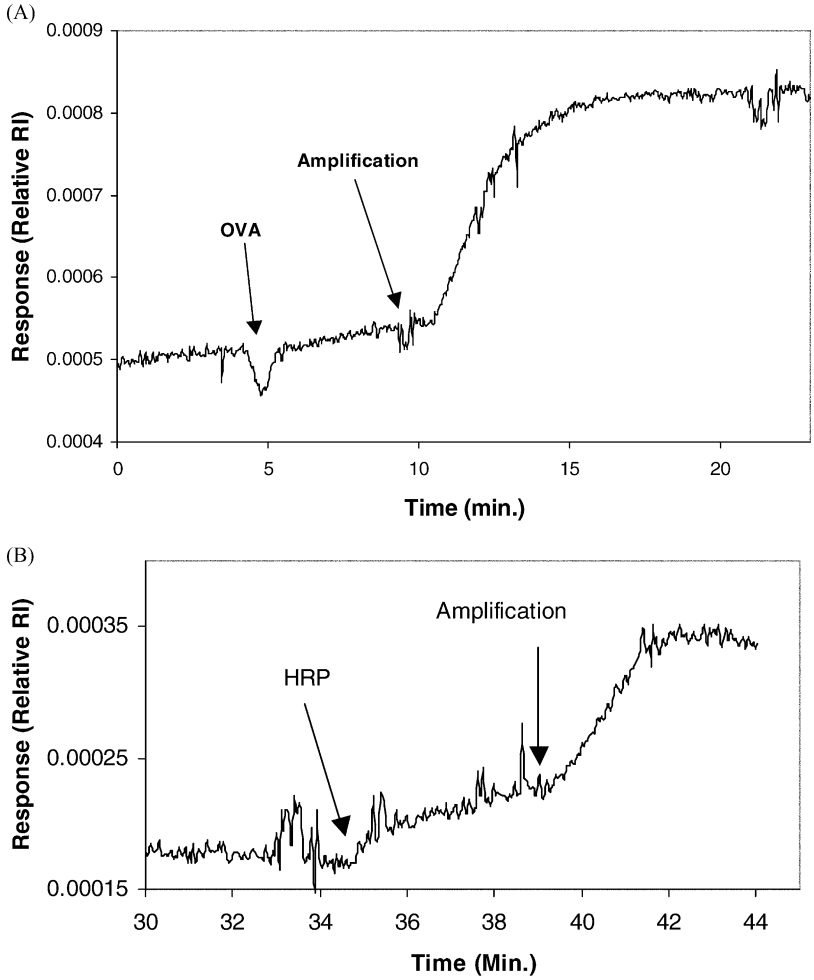

Fig. 10. Detection of ovalbumin (OVA) and horseradish peroxidase (HRP) at 1 nM concentration, 5 min primary detection time, 5 min amplification during the second flight. Response refers to relative refractive index units. (A) Reference compensated response of anti-OVA channel. OVA was acquired at time $t = 2$ min. It reached the sensor surface at time $t = 5$ min. Amplification was started at time $t = 10$ min. The sensor was washed with the buffer at time $t = 15$ min. (B) Reference compensated response of anti-HRP channel. HRP was introduced at time $t = 31$ min. At time $t = 34$ min it reached the sensor. At time $t = 39$ min amplification solution was introduced. The sensor was washed with the buffer solution at time $t = 43$ min.

chain and *botulinum* toxoid at nM levels with the laboratory prototype. The simulants chosen for the flights are in the same size range of the actual toxins.

For the second flight, the manual fluidics system that required user's actions to change solutions flowing through the sensor was replaced with computer-controlled rotary valve and pressurized containers with buffer, amplification and regeneration solutions (Fig. 4). Concentration of the introduced analytes was reduced from 10 to 1 nM, detection altitude was increased from 1800 to 6000 feet, and the detection time was reduced to 5 min. Detection of the same two analytes (OVA and HRP) is shown in Fig. 10. A 5 min detection of OVA was followed by an amplification/verification step (Fig. 10A). The 5 min detection of HRP was also followed by an amplification/verification step (Fig. 10B). The amplification/verification step not only increases the size of the signal but also eliminates false positives. This is a very important step during monitoring of actual chem/bioagents where avoidance of false positives is critical.

In addition to SPR detection, data important for unmanned flights were recorded and synchronized to the collected detection data. These data sets included: altitude, airspeed, angle of attack, GPS position, and meteorological data. Fig. 11 shows the plots of percent humidity, temperature and altitude as a function of time during flight 2. Fig. 12 shows the G-force and altitude as a function of time during flight 2.

A third flight included detection of a 1 nM OVA sample at 10,000 feet and regeneration of the sensor's surface and a second detection of OVA during the same flight (data not shown). The flight data are summarized in Table 1.

Some challenges specific to the airborne detection using SPR were anticipated before any flights began, while others were discovered during the three flights. Varying temperatures along flight path, subfreezing temperatures at high altitudes, air saturated sample solutions, and liquid in the collection stream were some of the problems that had to be addressed. Changes in temperature affect the materials of the SPR sensor and RI of aqueous sample solutions. Man-

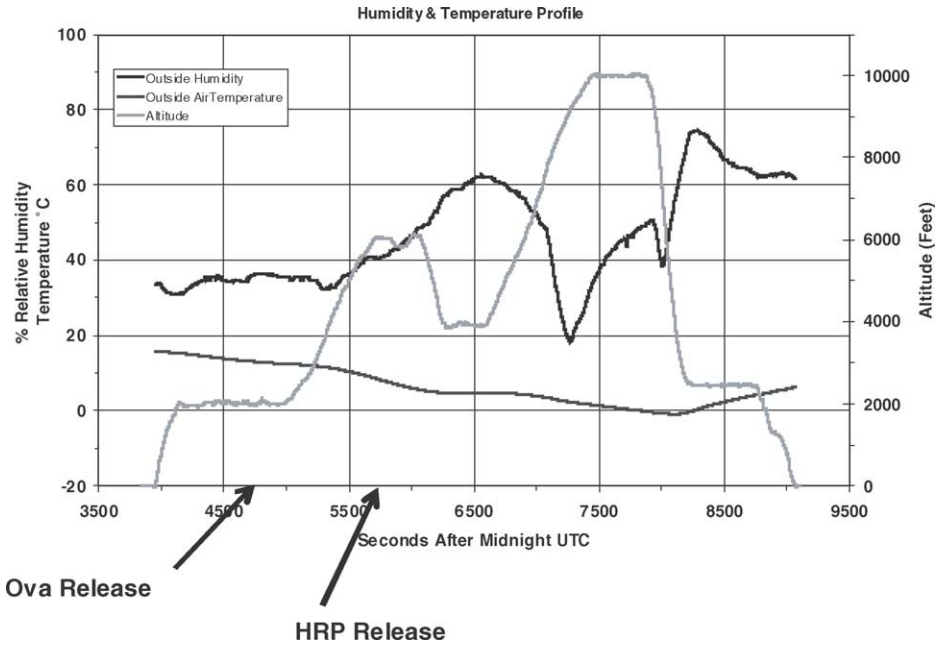

Fig. 11. Outside humidity, temperature and altitude during the flight (flight 2).

agement of the effects of temperature changes on the SPR signal was achieved by temperature stabilization and compensation [27]. The multi-channel design used here provided for the detection of two analytes, while using one channel to reference against the other. As noted above, inclusion of a third dedicated reference channel will prevent interference in the case where both analytes are present simultaneously. The reference channel also compensated for bulk RI changes, non-specific binding, and minor temperature variations, while the temperature controller provided the temperature stability necessary for monitoring small changes in RI.

Since air saturated samples can form bubbles which interfere with SPR measurements on the sensor surface, the debubbler was incorporated into the system. This in-line device was shown to be as effective at removing dissolved oxygen as 30 min of vacuum degassing in a test tube.

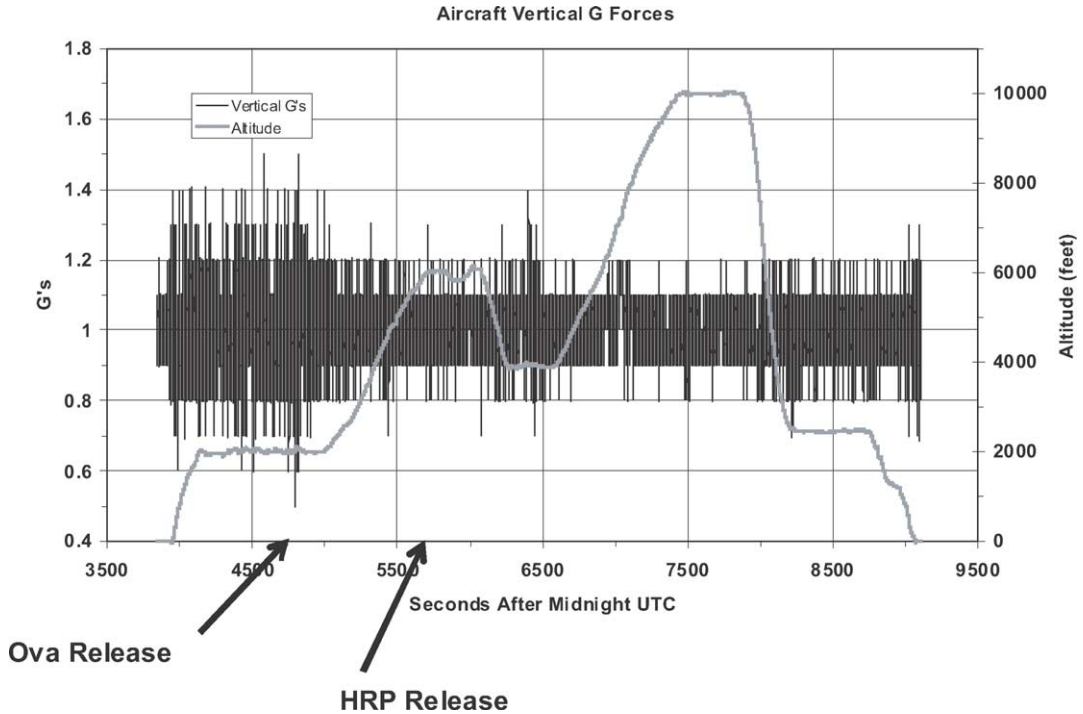

Fig. 12. Aircraft vertical G-forces and altitude during flight (flight 2).

Table 1
Summary of flight data

Flight number	Target concentration	Detection altitude (feet AGL[a])	Detection time (min)	Data collected	Targets attempted/detected
1	10 nM (0.6 μg/ml)	1700	15	SPR[b], GPS[c]	2/2 (100%)
2	1 nM (60 ng/ml)	2000–6000	5	SPR, GPS, Meteo[d], EFIS[e]	2/2 (100%)
3	1 nM (60 ng/ml)	10000	5	Meteo, SPR, GPS, EFIS (telemetry link tested)	2/2 (100%)

[a] Above ground level.
[b] Surface plasmon resonance.
[c] Global positioning system.
[d] Meterological data.
[e] Electronic flight instrumentation system.

4. Summary

The experiments and the instrumentation described above established that airborne BW agent detection is possible using the portable SPR system at the current level of technology development. The debubbler/deaerator effectively degassed samples and prevented bubble formation during the analyses. The adhesive mylar stencil worked well for sensor surface functionalization, and reduced reagent consumption compared with our earlier system of functionalizing sensor surfaces under flow conditions [12]. The computer-controlled fluidics unit reduced the dependence on the operator and set the stage for subsequent transition to unattended sensors. Detection experiments were performed during one ground test and three separate flights at several altitudes from 1800 to 10,000 feet. All analyte releases during the three flights were detected at all concentrations. In addition to bio-detection data meteorological and flight data of the type that will be useful for future UAV flights were recorded in flight for later analysis (Figs. 11,12). The aircraft position was tracked with a GPS unit and synchronized to the collected detection data. Combining detection data with aircraft position obtained by GPS allowed mapping the area where analytes were encountered. The SPR system mounted in the surrogate UAV demonstrated the usefulness of this technology for detection of airborne analytes.

Acknowledgements

This work was supported in part by a grant from the Department of Defense, by grant 62-4573 from Washington State Sea Grant. and by grant 66-0618 from Center for Process Analytical Chemistry, University of Washington.

References

[1] M. McDonnell, Biosensors in the detection of biological agents, NATO ASI Ser., Ser. E 252 (1993) 369–375.
[2] D.R. Franz, P.B. Jahrling, A.M. Friedlander, D.J. McClain, D.L. Hoover, W.R. Bryne, J.A. Pavlin, G.W. Christopher, E.M. Eitzen Jr., Clinical recognition and management of patients exposed to biological warfare agents, JAMA 278 (1997) 399–411.
[3] H.C. Lane, J.L. Montagne, A.S. Fauci, Bioterrorism: a clear and present danger, Nat. Med. 7 (2001) 1271–1273.
[4] H.C. Lane, A.S. Fauci, Bioterrorism on the home front: a new challenge for American medicine, JAMA 286 (2001) 2595–2597.
[5] F.S. Ligler, G.P. Anderson, P.T. Davidson, R.J. Foch, J.T. Ives, O.K.D. King, G. Page, D.A. Stenger, J.P. Whelan, Remote sensing using an airborne biosensor, Environ. Sci. Technol. 32 (1998) 2461–2466.
[6] G.P. Anderson, O.K.D. King, D.S. Cuttino, J.P. Whelan, F.S. Ligler, J.F. MacKrell, C.S. Bovais, D.K. Indyke, R.J. Foch, Biological agent detection with the use of an airborne biosensor, Field Anal. Chem. Technol. 3 (1999) 307–314.
[7] J. Davies (Ed.), Surface Analytical Techniques for Probing Biomaterial Processes, CRC Press, New York, 1996.
[8] P.O. Markgren, M. Hamalainen, U.H. Danielson, Screening of compounds interacting with HIV-1 proteinase using optical biosensor technology, Anal. Biochem. 265 (1998) 340–350.
[9] J. Homola, S.S. Yee, G. Gauglitz, Surface plasmon resonance sensors: review, Sens. Actuators B Chem. 54 (1999) 3–15.
[10] R.J. Green, R.A. Frazier, K.M. Shakesheff, M.C. Davies, C.J. Roberts, S.J. Tendler, Surface plasmon resonance analysis of dynamic biological interactions with biomaterials, Biomaterials 21 (2000) 1823–1835.
[11] J. Homola, J. Dostalek, S. Chen, A. Rasooly, S. Jiang, S.S. Yee, Reference-compensated surface plasmon resonance biosensor for detection of foodborne pathogens, Proc. SPIE-Int. Soc. Opt. Eng. 4416 (2001) 280–283.
[12] A.N. Naimushin, S.D. Soelberg, D.K. Nguyen, L. Dunlap, D. Bartholomew, J. Elkind, J. Melendez, C.E. Furlong, Detection of *Staphylococcus aureus* enterotoxin B at femtomolar levels with a miniature integrated two-channel surface plasmon resonance (SPR) sensor, Biosens. Bioelectron. 17 (2002) 573–584.
[13] G.C. Blanchard, C.G. Taylor, B.R. Busey, M.L. Williamson, Regeneration of immunosorbent surfaces used in clinical, J. Immunol. Meth. 130 (1990) 263–275.
[14] T. O'Brien, L.H. Johnson III, J.L. Aldrich, S.G. Allen, L.-T. Liang, A.L. Plummer, S.J. Krak, A.A. Boiarski, The development of immunoassays to four biological threat agents in a bidiffractive grating biosensor, Biosens. Bioelectron. 14 (2000) 815–828.
[15] P.A. Emanuel, J. Dang, J.S. Gebhardt, J. Aldrich, E.A. Garber, H. Kulaga, P. Stopa, J.J. Valdes, A. Dion-Schultz, Recombinant antibodies: a new reagent for biological agent detection, Biosens. Bioelectron. 14 (2000) 751–759.
[16] S. Koch, H. Wolf, C. Danapel, K.A. Feller, Optical flow-cell multichannel immunosensor for the detection of biological warfare agents, Biosens. Bioelectron. 14 (2000) 779–784.
[17] C.A. Rowe, L.M. Tender, M.J. Feldstein, J.P. Golden, S.B. Scruggs, B.D. MacCraith, J.J. Cras, F.S. Ligler, Array biosensor for simultaneous identification of bacterial, viral, and protein analytes, Anal. Chem. 71 (1999) 3846–3852.
[18] H. Yu, H. Ahmed, G.R. Vasta, Development of a magnetic microplate chemifluorimmunoassay for rapid detection of bacteria and toxin in blood, Anal. Biochem. 261 (1998) 1–7.

[19] K.A. Uithoven, J.C. Schmidt, M.E. Ballman, Rapid identification of biological warfare agents using an instrument employing a light addressable potentiometric sensor and a flow-through immunofiltration-enzyme assay system, Biosens. Bioelectron. 14 (2000) 761–770.
[20] W.E. Lee, H.G. Thompson, J.G. Hall, D.E. Bader, Rapid detection and identification of biological and chemical agents by immunoassay, Biosens. Bioelectron. 14 (2000) 795–804.
[21] K. Choi, W. Seo, S. Cha, J. Choi, Evaluation of two types of biosensors for immunoassay of botulinum toxin, J. Biochem. Mol. Biol. 31 (1998) 101–105.
[22] C.A. Rowe-Taitt, J.P. Golden, M.J. Feldstein, J.J. Cras, K.E. Hoffman, F.S. Ligler, Array biosensor for detection of biohazards, Biosens. Bioelectron. 14 (2000) 785–794.
[23] R.M. Wadkins, J.P. Golden, L.M. Pritsiolas, F.S. Ligler, Detection of multiple toxic agents using a planar array immunosensor, Biosens. Bioelectron. 13 (1998) 407–415.
[24] H. Yu, J.W. Raymonda, T.M. McMahon, A.A. Campagnari, Detection of biological threat agents by immunomagnetic microsphere-based solid phase fluorogenic- and electro-chemiluminescence, Biosens. Bioelectron. 14 (2000) 829–840.
[25] H. Yu, Comparative studies of magnetic particle-based solid phase fluorogenic and electrochemiluminescent immunoassay, J. Immunol. Meth. 218 (1998) 1–8.
[26] H. Yu, Enhancing immunoelectrochemiluminescence (IECL) for sensitive bacterial detection, J. Immunol. Meth. 192 (1996) 63–71.
[27] A.N. Naimushin, S.D. Soelberg, D. Bartholomew, J. Elkind, C.E. Furlong, A portable surface plasmon resonance (SPR) sensor system with temperature regulation, Sens. Actuators B Chem. 96 (2003) 253–260.
[28] R.G. Woodbury, C. Wendin, J. Clendenning, J. Melendez, J. Elkind, D. Bartholomew, S. Brown, C.E. Furlong, Construction of biosensors using a gold-binding polypeptide and a miniature integrated surface plasmon resonance sensor, Biosens. Bioelectron. 13 (1998) 1117–1126.
[29] J.V. Staros, R.W. Wright, D.M. Swingle, Enhancement by *N*-hydroxysulfosuccinimide of water-soluble carbodiimide-mediated coupling reactions, Anal. Biochem. 156 (1986) 220–222.
[30] Z. Grabarek, J. Gergely, Zero-length crosslinking procedure with the use of active esters, Anal. Biochem. 185 (1990) 131–135.